Thermo-optic plasmo-photonic mode interference switches based on dielectric loaded waveguides

K. Hassan,[1] J.-C. Weeber,[1,a)] L. Markey,[1] A. Dereux,[1] A. Pitilakis,[2] O. Tsilipakos,[2] and E. E. Kriezis[2]
[1]*Laboratoire Interdisciplinaire Carnot de Bourgogne, UMR 5209 CNRS-Université de Bourgogne, 9 avenue A. Savary, BP 47870, F-21078 Dijon, France*
[2]*Department of Electrical and Computer Engineering, Aristotle University of Thessaloniki, Thessaloniki GR-54124, Greece*

(Received 13 October 2011; accepted 28 November 2011; published online 14 December 2011)

We demonstrate an efficient thermo-optic dielectric loaded surface plasmon polariton waveguide (DLSPPW) 2×2 switch using a high thermo-optic coefficient polymer and a dual mode interference configuration. Unlike previous configurations relying on single-mode waveguide circuitry, the switch we consider is based on the interference between a plasmonic and a low-damping photonic mode of the DLSPPW, thus leading to the minimization of insertion losses of the device. Switching extinction ratios of 7 dB are measured for a compact 119 μm-long device. The overall device performances are in good agreement with numerical simulations performed using the beam propagation method. © *2011 American Institute of Physics*. [doi:10.1063/1.3670500]

Plasmonic technology is currently perceived as a disruptive approach for the integration of photonic and electronic functionalities on a single chip. In this context, the dielectric loaded surface plasmon polariton waveguides (DLSPPWs) is a promising candidate for the design of plasmonic circuitry. The properties of this plasmonic waveguide have been extensively investigated in recent years,[1–4] and its compatibility with the silicon-on-insulator guiding platform has been demonstrated.[5–7] Even more recently, DLSPPWs have been applied to high bit rate board-to-board optical interconnects and Gbps-throughput transmission along an hybrid silicon-DLSPPW platform.[6,7]

A DLSPPW is comprised of a dielectric guiding ridge loaded on top of a thin metal film. If a polymer with a large thermo-optical coefficient (TOC) is used as the loading material, the DLSPPW can be efficiently thermally controlled by using the metal film as the heating electrode. Several configurations of thermo-plasmonic switches using dual waveguide ring resonators,[8] Mach-Zehnder interferometers, and multi mode interferometers[9] have been numerically studied. Additionally, various thermally tunable DLSPPW components, such as modulators[10,11] and filters,[12] have been experimentally demonstrated.

All these experimentally demonstrated components operate in the single-mode regime, i.e., the waveguides support only the fundamental quasi-transverse magnetic (TM) polarized plasmonic mode. However, sufficiently wide DLSPPWs can support also a second-order mode with a large field component in the transverse-electric (TE) direction and an intensity peak, not situated at the metal/dielectric interface, but rather toward the center of the dielectric loading.[2,5,9] Owing to these properties, the second-order mode suffers smaller propagation losses than the quasi-TM fundamental mode and can be labeled as a photonic mode. Although identified for quite some time by several authors,[2,13] this mode has not yet been utilized in practical devices.

In this work, we report on an efficient and compact 2×2 plasmo-photonic switch relying on the interference of the fundamental plasmonic mode and the second-order mode identified as the photonic mode of the DLSPPW. Unlike previous plasmonic switch designs,[10] in our dual-mode configuration, the low-damping photonic mode contributes to the reduction of the insertion losses of the device. The samples we consider were fabricated by electron beam lithography applied on a cycloaliphatic acrylate polymer layer (thickness ~540 nm) spin-coated onto a gold strip (surface 3×15 mm^2, thickness of 60 nm) deposited onto a clean glass slide. Prior to the electron beam exposure, the polymer exhibits a high TOC of $\partial n/\partial T \sim -3 \times 10^{-4}$ K^{-1} (extracted from ellipsometry measurements) and a refractive index of 1.53 at telecom wavelengths (1500–1600 nm). Figures 1(a) and 1(b) show scanning electron microscopy (SEM) of a typical dual mode

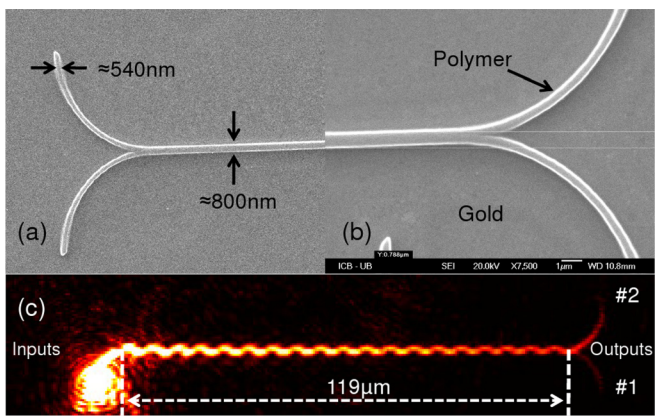

FIG. 1. (Color online) (a) (resp. (b)) SEM images of a typical DLSPPW DMI switch input (resp. output) made of cycloaliphatic acrylate polymer lying on a thin gold film. (c) LRM image of DMI switch at room temperature for a free-space wavelength of 1566 nm.

a)Electronic mail: jcweeber@u-bourgogne.fr.

interference (DMI) switch considered in this work. The DMI switch is comprised of an input (Fig. 1(a)) and output (Fig. 1(b)) Y-junction connected to a 119 μm-long DMI waveguide. By injecting a current through the gold film, the polymer is heated, and the effective indices $n_{\text{eff}}^{(1)}$ and $n_{\text{eff}}^{(2)}$ of the two modes traveling along the DMI region are changed. This change modifies the beating length of the two interfering modes and eventually switching is achieved provided that the DMI waveguide is of sufficient length.[9] The optimum DMI length L is given by $2L = \lambda/|\Delta n_{\text{eff}}^{(1)} - \Delta n_{\text{eff}}^{(2)}|$, where λ is the free-space wavelength at the frequency of interest and where $\Delta n_{\text{eff}}^{(1,2)}$ denotes the effective index change for each mode when switching from the unheated (cool) to the heated (hot) state. If the DMI waveguide length is an even (or odd) multiple of the beating length, then the switch will operate in the BAR (or CROSS) state. Figure 1(c) shows a leakage radiation microscopy (LRM) image of the beating pattern (period $L_B \simeq 3\mu$m) in the cool (room temperature) state for $\lambda_0 = 1566$ nm. The input beam is focused on the bottom-left input port and exits through the upper-right output port, i.e., the switch operates in the CROSS state. The two input/output ports of the Y-junctions are made of arced (10 μm-radius) single-mode DLSPPW with a 540 nm-wide polymer ridge, whereas the DMI region is a polymer ridge with a width of $w \simeq 800$ nm carefully designed in order to ensure that only two guided modes are supported in both hot and cool states.[9] The two modes supported by the DMI region are the fundamental DLSPPW mode and the second order mode, respectively, labeled TM_{00} and TE_{00} hereafter. The TM_{00} mode is naturally the fundamental plasmonic mode, whereas the second-order TE_{00}, as discussed earlier, resembles more the photonic mode. Moreover, for the particular dimensions considered here, the TM_{00} and TE_{00} have cross-sectional electric field distributions of opposite symmetry (symmetric and anti-symmetric, respectively) for the component normal to the metal. Note that unlike a pure photonic mode, the TE_{00} mode we consider here has a significant electric field component in the direction perpendicular to the metal film.[9] Consequently, provided that the input waveguide is laterally shifted compared to the DMI axis, the incident TM_{00} mode can excite equally well the two DMI waveguide modes, thus giving raise to the mode-beating employed for the switching.[9] The LRM images of the output ports of the device are displayed in Figs. 2(a) and 2(b), for the cool and hot states, respectively. In this experiment, the hot state is obtained by injecting a 400 mA DC current through the gold film (cross-section $3000 \times 0.06\ \mu\text{m}^2$). According to a reading of a shielded micro thermocouple placed in contact with the metal film at a distance of a few millimeters from the waveguides, the heating current induces a temperature raise in the polymer in the order of $\Delta T \simeq 60$K. At a given wavelength, the input and output optical power levels are obtained by integrating the intensity of the corresponding LRM image over areas of interest located, respectively, at the input and the output ports.[12] By sweeping the incident wavelength from 1500 to 1600 nm and by normalizing the output signal to the input, the transmission spectra plotted on Fig. 2(c) have been obtained. For both temperature states, differences between the highest and the lowest transmission levels larger than −20 dB are achievable. Note that for both temperature

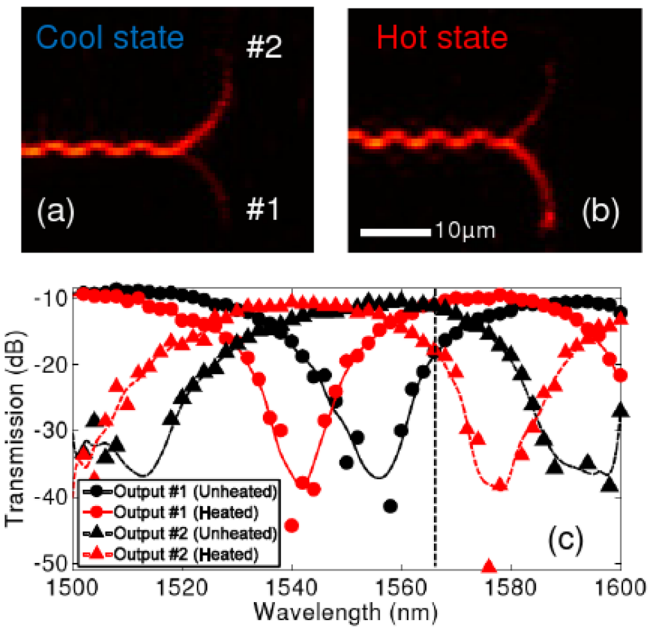

FIG. 2. (Color online) (a) LRM image (1566 nm) of the device output at the cold state. (b) Same as (a) in the hot state. (c) Experimentally measured transmission spectra at the two DMI switch output ports, for the cold and hot states.

states, the insertions losses are lower than −10 dB for a device with a total length up to 150 μm. Compared to a straight single-mode waveguide of equal length, where an attenuation of at least −15 dB is expected, the damping along the DMI region is rather moderate. This is due to the fact that in the DMI waveguide the guided power is split between the two supported modes, and the second-order mode of the DMI (TE_{00}) has lower propagation-losses compared to the fundamental DLSPPW mode (TM_{00}).[9] Indeed, for the DMI we consider here, the TE_{00} mode has a $1/e$ damping distance at 1550 nm ($L_{spp} = 100\ \mu$m) more than two times larger than for the TM_{00} modes ($L_{spp} = 45\ \mu$m). However, for DMI waveguides of moderate length (around 100 μm), this difference does not impact sufficiently the amplitude of the mode beating to inhibit the switching effect. For symmetric 2×2 switch operation, the switch extinction ratio (ER) (i.e., the ratio between the transmission levels when switching from the cool to the hot state) of each output port should be of equal magnitude and of opposite sign. These conditions apply for the wavelength of 1566 nm leading to an ER around 7 dB (see vertical line in 2(c)). Note that for a given length of the DMI waveguide, the wavelength leading to a symmetric switch effect could be slightly adjusted by offsetting the temperature of the cool state.

The beating patterns and the measured transmission spectra acquired from the experimental setup have been compared to the ones produced by our finite-element beam propagation method (FE-BPM).[14] The FE-BPM is a numerical tool very well adapted to the modeling of long axially arranged components such as the DMI switch. Employing the same structural and thermo-optical parameters as the ones of the fabricated sample, the numerical investigations retrieved the same qualitative aspects. Figure 3(a), depicts the numerically calculated beating pattern of the electric-field intensity, for a DMI length of 119 μm, at the cool state

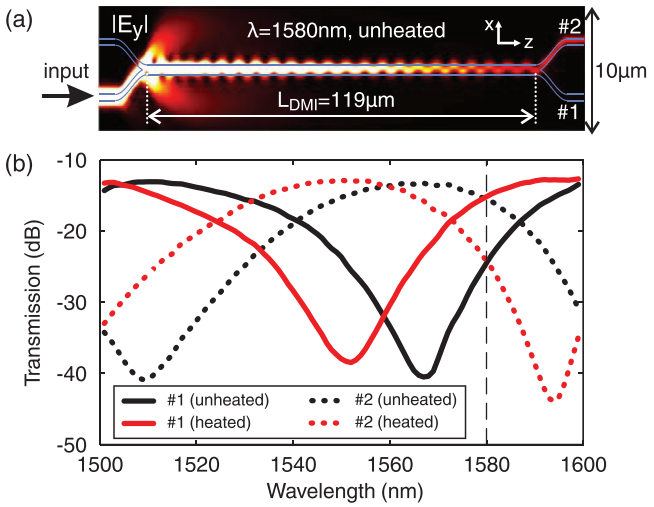

FIG. 3. (Color online) (a) Computed intensity beating pattern of the electric field component perpendicular to the metal film (axes not to scale). The DMI length is 119 μm, the polymer layer is in the cool state and $\lambda = 1580$ nm. Light is launched on the lower input port and is directed toward the opposite output-port # 2. (b) Transmission spectra for the cold and hot states, at the two output-ports for a temperature increase of $\Delta T = 15$ K.

and for a wavelength of 1580 nm. The FE-BPM transmission spectra of Fig. 3(b) reveal an optimum switch ER of 9 dB at 1580 nm for a temperature increase of $\Delta T = 15$ K, a free spectral range (FSR) of 90–100 nm and insertion losses of $\sim$10 dB. Noting that the red-shift of about 15 nm observed in the simulated spectra originates from acceptable deviations in the fabricated sample dimensions, these spectral features are in good agreement with the experimental ones. We note however that the theoretical temperature difference ΔT necessary to achieve the switching is clearly underestimated compared to the experimental value. This difference is attributed to a poor estimate of the waveguides temperature with the remotely located micro thermocouple.

To summarize, we have reported on the fabrication and experimental demonstration of a thermo-optic 2×2 switch based on dual-mode DLSPPWs, supporting both the fundamental (or plasmonic) and the second-order (photonic) mode. The switching configuration is based on a DMI design where the thermal tuning of the beating-length created by the interference of the plasmonic and the photonic mode in the dual mode waveguide is employed for the switching. Output-port extinction ratios of $\sim$7 dB have been measured in a 119 μm-long DMI symmetric switch, while insertions losses below -10 dB are obtained owing to the contribution of the moderate damping of the photonic mode. The overall device experimental performances are found in good agreement with numerical simulation predictions. The thermal modeling of the device[15] indicates a switching time of $\simeq 1\mu$s with this configuration, when using finite width electrodes instead of a macroscopic gold strip. The evaluation of such a switch for the routing of high-bit rate signals is in progress and will be reported elsewhere.

This work is part of the European FP7 research program PLATON, Contract Number 249135.

[1]B. Steinberger, A. Hohenau, H. Ditlbacher, A. L. Stepanov, A. Drezet, F. R. Aussenegg, A. Leitner, and J. R. Krenn, Appl. Phys. Lett. **88**, 094104 (2006).
[2]S. Massenot, J. Grandidier, A. Bouhelier, G. Colas des Francs, L. Markey, J.-C. Weeber, A. Dereux, J. Renger, M. U. Gonzalez, and R. Quidant, Appl. Phys. Lett. **91**, 243102 (2007).
[3]T. Holmgaard, S. Bozhevolnyi, L. Markey, A. Dereux, A. Krasavin, P. Bolger, and A. Zayats, Phys. Rev. B **78**, 165431 (2008).
[4]J. Grandidier, S. Massenot, G. des Francs, A. Bouhelier, J.-C. Weeber, L. Markey, A. Dereux, J. Renger, M. González, and R. Quidant, Phys. Rev. B **78**, 245419 (2008).
[5]R. M. Briggs, J. Grandidier, S. P. Burgos, E. Feigenbaum, and H. A. Atwater, Nano Lett. **10**, 4851 (2010).
[6]D. Kalavrouziotis, G. Giannoulis, D. Apostolopoulos, S. Papaioannou, A. Kumar, S. Bozhevolnyi, L. Markey, K. Hassan, J.-C. Weeber, A. Dereux *et al.*, *Proceedings of ECOC 2011, Geneva, 18 September 2011, OSA Technical Digest (CD)*, (Optical Society of America, Washington, DC, (2011), paper We.10.P1.27.
[7]S. Papaioannou, C. Vyrsokinos, O. Tsilipakos, A. Pitilakis, K. Hassan, J.-C. Weeber, L. Markey, A. Dereux, S. Bozhevolnyi, A. Miliou *et al.*, J. Lightwave Technol. **29**, 3185 (2011).
[8]O. Tsilipakos, E. E. Kriezis, and S. S. I. Bozhevolnyi, J. Appl. Phys. **109**, 073111 (2011).
[9]A. Pitilakis and E. E. Kriezis, J. Lightwave Technol. **29**, 2636 (2011).
[10]J. Gosciniak, S. I. Bozhevolnyi, T. B. Andersen, V. S. Volkov, J. Kjelstrup-Hansen, L. Markey, and A. Dereux, Opt. Express **18**, 1207 (2010).
[11]S. Randhawa, A. V. Krasavin, T. Holmgaard, J. Renger, S. I. Bozhevolnyi, A. V. Zayats, and R. Quidant, Appl. Phys. Lett. **98**, 161102 (2011).
[12]K. Hassan, J.-C. Weeber, L. Markey, and A. Dereux, J. Appl. Phys. **110**, 023106 (2011).
[13]T. Holmgaard and S. I. Bozhevolnyi, Phys. Rev. B **75**, 245405 (2007).
[14]O. Tsilipakos, A. Pitilakis, A. Tasolamprou, T. Yioultsis, and E. Kriezis, Opt. Quantum Electron. **42**, 541 (2011).
[15]O. Tsilipakos, T. V. Yioultsis, and E. E. Kriezis, J. Appl. Phys. **106**, 093109 (2009).